

## Choking of electron flow: A mechanism of current saturation in field-effect transistors

M. I. Dyakonov\* and M. S. Shur

*Department of Electrical Engineering, University of Virginia, Charlottesville, Virginia 22903-2442*

(Received 6 September 1994; revised manuscript received 6 February 1995)

We describe a mechanism of the current saturation in a field-effect transistor (FET) caused by *choking* of electron flow. The choking occurs when the electron velocity at the drain side of the channel reaches the plasma-wave velocity. This effect is quite similar to the choking of a gas flow in a pipe. This mechanism is an alternative to the well-known mechanism of current saturation caused by the drift velocity saturation in the FET channel. We show that the choking mechanism may dominate in a submicrometer  $\text{Al}_x\text{Ga}_{1-x}\text{As}/\text{GaAs}$  FET at 10 K and low drain and gate bias voltages.

### I. INTRODUCTION

When the mean free path for electron-electron collisions is much smaller than the sample length and the electron mean free path for collisions with impurities and phonons, electrons behave like a fluid which may be described by hydrodynamic equations. In our recent paper,<sup>1</sup> we showed that this condition can be met for two-dimensional (2D) electrons in a field-effect transistor (FET), and that the hydrodynamic equations describing this electron fluid coincide with those for shallow water. In this analogy the plasma waves in the FET channel play the role of shallow water waves. We also showed that in a short enough device an instability should occur at a relatively small dc current because of spontaneous plasma-wave generation. This provides a mechanism for the emission of tunable far-infrared electromagnetic radiation.

In this work, we demonstrate that hydrodynamic properties of electrons in a FET may lead to a mechanism of the drain current saturation (different from the two conventional mechanisms—the channel pinchoff and the drift velocity saturation). This mechanism is related to the effect of *choking* of the electron fluid, similar to the choking of a gas flow in a pipe. The choking of the gas flow occurs when its velocity approaches the sound velocity at the downstream end of the pipe.<sup>2</sup> When this condition is reached, the flux saturates: it cannot be increased further by a decrease of the pressure at the downstream end of the pipe. The choking of the electron flow should take place when the electron velocity reaches the plasma-wave velocity. As we show in this paper, the choking phenomenon in short samples should lead to a large change in the current-voltage characteristics.

Our approach based on the “shallow water” hydrodynamic equations allows us to describe the FET characteristics for both long and short (ballistic) devices. In the latter case, our theory predicts a much smaller saturation current than conventional theories.

As we mentioned above, the laws of hydrodynamics apply when the mean free path for interelectronic collisions,  $\lambda_{ee}$ , is much smaller than both the device length  $L$  and the mean free path for electron collisions with phonons and/or impurities,  $\lambda$  (which determine the electron

mobility). The value of  $\lambda$  depends on relevant scattering mechanisms and may vary for GaAs-based FET's from  $\sim 0.1 \mu\text{m}$  or less at room temperature to a micrometer or more at cryogenic temperatures. The value of  $\lambda_{ee}$  depends on the Fermi energy  $E_F$ , the thermal energy  $kT$ , and the Bohr energy  $E_B = e^4 m / (2\epsilon_s^2 \hbar^2)$ , where  $m$  is the electron effective mass,  $\epsilon_s$  is the semiconductor dielectric constant, and  $\hbar$  is the Planck constant. If  $kT$  or  $E_F$ , whichever is larger, is much greater than  $E_B$ , the electrons may be regarded as an ideal gas. In this case,  $\lambda_{ee}$  is much larger than the interelectronic distance  $n_s^{-1/2}$  where  $n_s$  is the sheet electron concentration. In the case when  $kT \approx E_F \approx E_B$ , the electrons form a highly nonideal gas where  $\lambda_{ee}$  is of the same order as the interelectronic distance. For the Fermi-liquid case, i.e.,  $kT \ll E_F \approx E_B$ , electron-electron collisions are suppressed (due to the Pauli principle) and  $\lambda_{ee}$  drastically increases with decreasing  $kT$ .<sup>3</sup>

As we discussed in Ref. 1, an  $\text{Al}_x\text{Ga}_{1-x}\text{As}/\text{GaAs}$  heterostructure field-effect transistor (HFET) with  $n_s \approx 10^{12} \text{cm}^{-2}$  at 77 K and  $L \approx 0.2 \mu\text{m}$  is an example of a device where the hydrodynamics approach is justified. Therefore many hydrodynamic phenomena such as wave propagation, shock waves, turbulence, solitons, etc. may take place in the 2D electron fluid in such a FET. In the hydrodynamic equations for the 2D electrons coinciding with those for shallow water, the gate-to-channel voltage plays the role of the water level and the plasma waves in the FET channel play the role of shallow water waves.

This similarity extends to an interesting hydrodynamic phenomenon called choking. Even though the choking effect may occur in a shallow water flow,<sup>4</sup> it is easier to understand this effect by considering a classic problem of gas flow in a pipe with a constant cross section where the friction between the flow and the walls of the pipe is important (see Fig. 1). For a subsonic flow, the friction leads to a pressure drop along the channel [see Fig. 1(a)]. As the pressure drops so does the gas density. Since the flux along the pipe must remain constant, the hydrodynamic velocity has to rise. Eventually it may reach the sound velocity  $s$  at the downstream end of the pipe. Once this happens, the flux saturates and remains constant with further increase in pressure difference along the

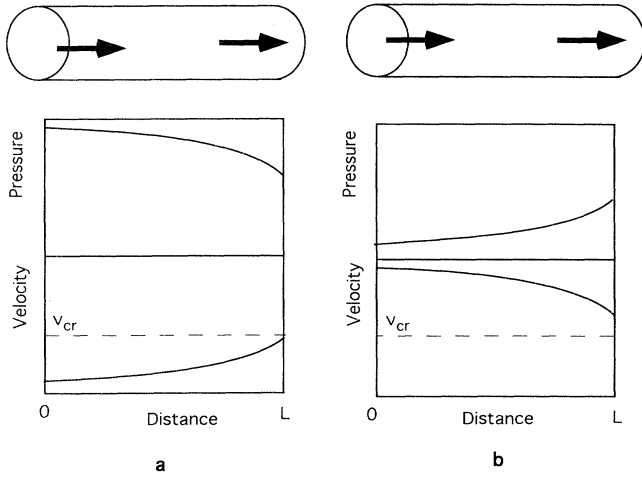


FIG. 1. Schematic distributions of pressure and velocity for subsonic (a) and supersonic (b) gas flows in a pipe with friction.

pipe. If the flow enters the pipe with a supersonic velocity, then pressure rises and velocity decreases along the pipe [see Fig. 1(b)].

In a FET, the role of the sound velocity is played by the plasma wave velocity  $s = (eU/m)^{1/2}$ , where  $e$  is the elementary charge,  $m$  is the electron effective mass, and  $U$  is the gate-channel voltage swing. (Here we assume that  $U > kT/e, E_F/e$ . Otherwise,  $s$  becomes of the order of the thermal velocity or the Fermi velocity.) Once the electron velocity reaches  $s$  at the drain, the choking effect occurs, leading to the drain current saturation. The competing mechanism is the drift velocity saturation at the drain side of the channel. Hence the choking may occur if  $s < v_{\text{sat}}$ , where  $v_{\text{sat}}$  is the electron saturation velocity.

If choking does occur, it may strongly affect the current-voltage characteristics. This will happen if the plasma-wave velocity is much smaller than the average drift velocity in the channel at pinchoff predicted by the conventional theory:  $s_s = (eU_s/m)^{1/2} \ll \mu U_s/L$ , where  $U_s$  is the gate-to-source voltage swing. In the opposite limiting case, the exact value of the electron velocity at the drain does not affect the saturation voltage or the saturation current. (This condition is very similar to the condition  $v_{\text{sat}} \ll \mu U_s/L$  which has to be fulfilled for the electron velocity saturation to strongly affect the current-voltage characteristics; see, for example, Ref. 5.)

The inequality  $s_s \ll \mu U_s/L$  can be rewritten as

$$L \ll s\tau, \quad (1)$$

where  $\tau$  is the momentum relaxation time. Equation (1) specifies the condition under which the current-voltage characteristic is strongly affected by choking. As will be shown below, this condition can be met in  $\text{Al}_x\text{Ga}_{1-x}\text{As}/\text{GaAs}$  HFET's at low temperatures for devices with submicrometer gate lengths and for small gate voltage swings.

In this paper, we will limit ourselves to the case when  $U_s > kT/e$  (this corresponds to the above-threshold regime of operation). However, we can show that the choking phenomenon may take place in the subthreshold

regime as well, except that in this case the plasma waves become the sound waves in the electronic fluid, and  $s$  is on the order of the thermal velocity  $v_{\text{th}} = (kT/m)^{1/2}$  or of the order of the Fermi velocity  $v_F$ .

## II. BASIC EQUATIONS

We start from the hydrodynamic equations for the 2D electrons derived in Ref. 1 where we add a dissipative term  $-v/\tau$  which describes the electron collisions with impurities and/or phonons:

$$\frac{\partial v}{\partial t} + v \frac{\partial v}{\partial x} = -\frac{e}{m} \frac{\partial U}{\partial x} - \frac{v}{\tau}. \quad (2)$$

Here  $U = U_{gc}(x) - U_T$ ,  $U_{gc}(x)$  is the local gate-to-channel voltage swing,  $U_T$  is the threshold voltage,  $\partial U/\partial x$  is the longitudinal electric field in the channel, and  $v(x, t)$  is the local hydrodynamic electron velocity. Equation (2) is the Euler equation of motion which has to be solved together with the continuity equation

$$\frac{\partial U}{\partial t} + \frac{\partial(Uv)}{\partial x} = 0, \quad (3)$$

where we use the usual gradual channel approximation for the surface electron concentration  $n_s = CU/e$ . Here  $C$  is the gate capacitance per unit area. (This relationship between  $n_s$  and  $U$  is valid as long as  $U > kT/e$ .)

In steady state, Eq. (3) becomes  $U = j/(Cv)$  where  $j$  is the current per unit gate width and Eq. (2) reduces to

$$\left[ \frac{v_{\text{cr}}^3}{v^3} - 1 \right] \frac{dv}{dx} = \frac{1}{\tau}, \quad (4)$$

where we introduce the critical velocity  $v_{\text{cr}} = (ej/mC)^{1/3}$  (similar to the critical flow velocity in gas dynamics). Using dimensionless voltage  $u = U/U_0$ , current  $i = j/j_0$ , velocity  $w = v\tau/L$ , and coordinate  $\xi = x/L$ , where  $U_0 = m(L/\tau)^2/e$  and  $j_0 = Cm(L/\tau)^3/e$  and integrating Eq. (4), we obtain

$$\frac{i}{2w_s^2} - \frac{i}{2w^2} + w_s - w = \xi, \quad (5)$$

where  $w_s = i/u_s$  is the velocity at the source end of the channel,  $u_s = U_s/U_0$ , and  $U_s = U(0)$  is the value of the gate voltage swing at the source. Equation (5) is a cubic equation with respect to  $w$ . Hence, for a given value of  $j$ , this equation has three solutions and for one of them  $w$  is negative. The negative solution is unphysical, since for positive  $j$  it corresponds to a negative electron concentration.

For  $\xi = 1$ , we have  $u = u_d = U_d/U_0$  where  $U_d = U(L)$  is the value of the gate voltage swing at the drain, and Eq. (5) may be rewritten as

$$i^2 \left[ \frac{1}{u_d} - \frac{1}{u_s} \right] + i - \frac{1}{2}(u_s^2 - u_d^2) = 0. \quad (6)$$

Equation (6) gives the current-voltage dependence. Differentiating this equation with respect to  $u_d$  and putting  $di/du_d = 0$ ,  $i = i_{\text{sat}}$ , we find the relationship between the saturation current and the drain voltage swing:

$$i_{\text{sat}} = u_d^{3/2}. \quad (7)$$

This equation also follows from the fact that at the saturation point the velocity at the drain is equal to the plasma-wave velocity  $s$ .

Substituting  $u_d$  from Eq. (7) into Eq. (6) and letting  $i = i_{\text{sat}}$ , we obtain the relationship between the saturation current  $i_{\text{sat}}$  and the gate voltage  $u_s$ :

$$i_{\text{sat}} + \frac{3}{2} i_{\text{sat}}^{4/3} - \frac{i_{\text{sat}}^2}{u_s} = \frac{u_s^2}{2}. \quad (8)$$

### III. RESULTS AND DISCUSSION

Figure 2 shows the dimensionless concentration  $u$  and channel potential  $u_s - u$  and velocity  $w$  versus the dimensionless distance  $\xi$  for three values of  $i$ . For each value of  $i$ , these profiles [which were obtained using Eq. (5) and letting  $u_s = 0.4$ ] have two branches which coincide at  $v = v_{\text{cr}}$  where the derivative  $dv/dx$  (or  $dw/d\xi$ ) diverges. Dashed lines in the figure correspond to the values of  $x$  outside the sample ( $x > L$ ) and hence are unphysical. The top branches in Fig. 2(a) and the bottom branches in Figs. 2(b) and 2(c) correspond to the solutions such that the concentration gradually decreases and the velocity

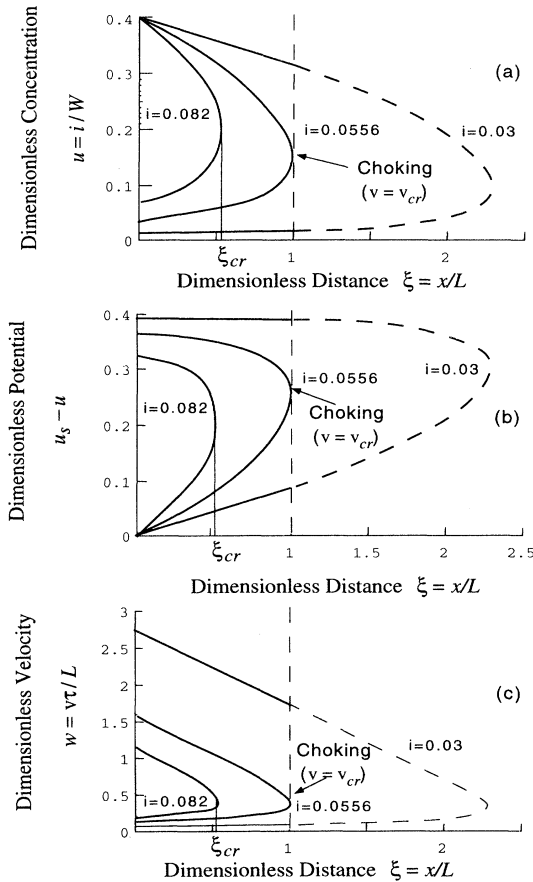


FIG. 2. Dimensionless concentration, potential, and velocity profiles in 2D electron fluid for different dimensionless currents.

and potential gradually increase from the source towards the drain along the channel. The bottom branches in Fig. 2(a) and the top branches in Figs. 2(b) and 2(c) correspond to the solutions such that the concentration gradually increases and the velocity and potential gradually decrease from the source towards the drain along the channel. These solutions describe the situation when electrons enter the channel from the source with a supersonic velocity ( $v > v_{\text{cr}}$ ) and then are slowed down by the negative potential difference (i.e., by a retarding electric field) along the channel. Thus the energy absorbed in the device for positive current and negative source-drain voltage comes from the kinetic energy of the incoming electrons. We should notice that for these branches  $u(0) < u_s$ . Mathematically, this occurs because Eq. (5) depends not on  $w_s = i/u_s$  but rather on  $i/w_s^2 + w_s$ . Physically, the combination of the top and bottom branches describes two types of shock waves which are well known in conventional hydrodynamics. The first type is described in the region near the source by the subsonic solution [corresponding to the top branch of Fig. 2(a) and to the bottom branches in Figs. 2(b) and 2(c)] and by a jump, somewhere in the middle of the channel, to the supersonic solution [corresponding to the bottom branch of Fig. 2(a) and to the top branches in Figs. 2(b) and 2(c)] which describes the carrier velocity, potential, and concentration profiles in the region from the jump up to the drain. However, using the results of conventional hydrodynamics, one can show that such a shock wave is not possible since this solution violates the second law of thermodynamics.<sup>6</sup> As can be seen from the figure and Eqs. (4) and (5), for the subsonic branches, the velocity at the source,  $v(x=0)$ , is smaller than  $v_{\text{cr}}$  and increases towards the drain (but does not surpass  $v_{\text{cr}}$ ). The second type of shock wave is described in the region near the source by the supersonic solution [corresponding to the bottom branch of Fig. 2(a) and to the top branches in Figs. 2(b) and 2(c)] and by a jump somewhere in the middle of the channel to the subsonic solution [corresponding to the top branch of Fig. 2(a) and to the bottom branches in Figs. 2(b) and 2(c)]. This second type of shock wave may exist.<sup>6</sup>

For  $v < v_{\text{cr}}$ , the velocity at the drain ( $x=L$ ) increases with current  $j$  until it reaches the critical velocity  $v_{\text{cr}}$ . When  $v(L) = v_{\text{cr}}$  [see curve for  $i = 0.056$  in Fig. 2(c)], the voltage swing at the drain,  $U(L)$ , is such that the local plasma-wave velocity at the drain  $s(L) = [eU(L)/m]^{1/2}$  becomes equal to  $v_{\text{cr}}$ . Since the value  $v_{\text{cr}}$  cannot be surpassed, the device current-voltage characteristic should saturate. This is completely analogous to the choking of a subsonic gas flow.<sup>2</sup>

However, we should point out that for currents higher than the choking saturation current Eq. (5) still has solutions for some range of values of  $0 < x < x_{\text{cr}}$  (see curves for  $i = 0.082$  in Fig. 2). Outside this range, no stationary solutions of Eqs. (2) and (3) exist. It means that for  $x_{\text{cr}} < x < L$  at least some of the assumptions used to derive these equations, such as the gradual channel approximation, for example, become invalid. A similar situation occurs in a conventional FET theory where the gradual channel approximation becomes invalid beyond

the point in the channel where the velocity saturates.<sup>5</sup>

Figure 3 shows the current-voltage dependence following from Eq. (6). For comparison, we also show the conventional result for the constant mobility model (i.e.,  $v_s$  tending to infinity, where  $v_s$  is the electron saturation velocity). The positive and negative voltage branches correspond to  $v < v_{cr}$  and to  $v > v_{cr}$ , respectively. The negative voltage branch is difficult to reproduce in Fig. 3(a), since it corresponds to very high currents, and therefore it is omitted. The dashed parts of the curves correspond to the shock-wave solutions discussed in relation to Fig. 2. (For the positive branch in Fig. 3, such shock waves cannot exist, and hence the dashed part of this curve is unphysical.) The negative branch cannot be realized in a FET with a typical  $n^+$  source contact since it requires the entering electron flow at the source to have a velocity greater than the plasma-wave velocity ( $v > s$ ). However, just as in gas dynamics, this branch of the solution may be realized in a specially designed FET structure similar to the well-known Laval nozzle<sup>2,4,6</sup> which produces a supersonic flow.

We should mention that Eq. (6) also has solutions corresponding to a negative current. These parts of the current-voltage characteristics (which are not shown in Fig. 3) correspond to conditions in which source and drain are interchanged, and the drain voltage is fixed.

The key parameter of our theory is  $u_s = (s\tau/L)^2$ ; see Eq. (1). Depending on the value of  $u_s$ , we distinguish between long ( $u_s \ll 1$ ) and short samples ( $u_s \gg 1$ ). According to this definition whether the sample is long or short depends not only on the actual sample length  $L$ , but also on the gate voltage swing (which defines the plasma-

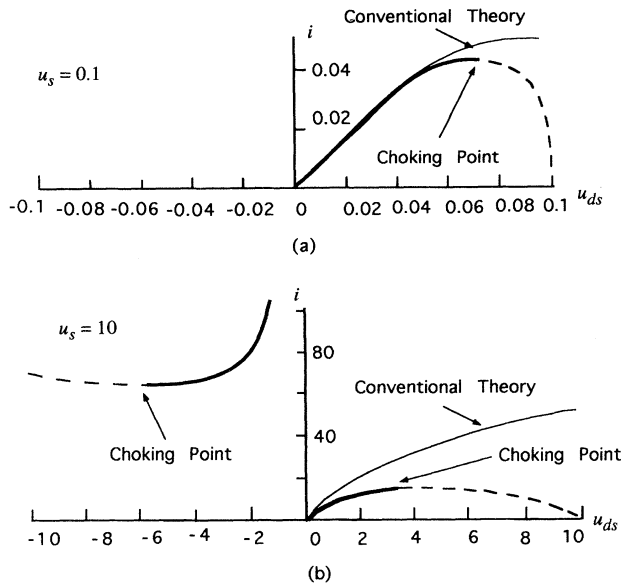


FIG. 3. Calculated dimensionless current-voltage FET characteristics for  $u_s = 0.1$  (a) and  $u_s = 10$  (b).  $u_{ds} = u_s - u_d$  is the dimensionless drain-source voltage. The conventional theory results are also presented. The "supersonic" branch at negative voltages for  $u_s = 0.1$  corresponds to very high currents and is omitted in (a). Dashed lines correspond to shock-wave solutions.

wave velocity  $s$ ). In a long sample, where Eq. (1) is not valid and  $u_s \ll 1$  [see Fig. 3(a)] the obtained  $I$ - $V$  characteristics are not very different from the conventional  $I$ - $V$  characteristics reviewed in many textbooks (see, for example, Ref. 5). The analysis of Eq. (8) shows that in a short sample [ $u_s \gg 1$ , see Fig. 3(b)] the saturation voltage and current are much smaller than those predicted by the conventional theory. This is clearly seen from Fig. 4 which compares the dependencies of the saturation voltage and the saturation current on the gate voltage swing predicted by the conventional theory and by the present theory [see Eqs. (7) and (8)].

The mechanism of current saturation caused by choking is an alternative to the well-known mechanism of current saturation caused by the drift velocity saturation in the FET channel. Our mechanism may be important if the velocity of waves propagating in the 2D electron system,  $s$ , is less than the saturation velocity  $v_{sat}$ . As we mentioned above, the velocity  $s$  being equal to  $(eU/m)^{1/2}$  for  $U \gg kT, E_F$  becomes equal to  $v_{th}$  or  $v_F$  if  $U \ll kT, E_F$ . Thus for the choking phenomenon to occur it is necessary that  $v_{th}, v_F \ll v_{sat}$ . This means that the current saturation due to choking should take place at low temperatures and low electron concentrations.

At 10 K, in GaAs,  $v_{sat} \approx 4v_{th} \approx 2 \times 10^7$  cm/s. By adjusting the gate bias in an  $Al_xGa_{1-x}As/GaAs$  HFET, we may choose the Fermi energy  $E_F$  to be of the same order as the thermal energy  $kT$  so that the 2D electron gas in the HFET channel is not strongly degenerate and the Fermi velocity does not exceed the thermal velocity. This corresponds to  $n_s \approx 3 \times 10^{10}$  cm<sup>-2</sup>. Then both  $E_F$  and  $kT$  are much less than the Bohr energy ( $\approx 7$  meV). Thus the electron gas is highly nonideal and the mean free path is roughly equal to the interelectronic distance  $(n_s)^{-1/2} \approx 600$  Å. Under such conditions and with gate voltages on the order of several millivolts, the choking effect will strongly affect the current-voltage characteristics for devices with gate lengths shorter than  $s\tau \approx 1$  μm for  $\tau \approx 20$  ps (which corresponds to the mobility  $\approx 500\,000$  cm<sup>2</sup>/V s). As follows from the estimates given above, the measurements of the current-voltage characteristics of deep submicrometer  $Al_xGa_{1-x}As/GaAs$  HFET's at voltages close to the threshold voltage should provide experimental evidence of the choking regime. (To our knowledge, no experiments have been done under such conditions.)

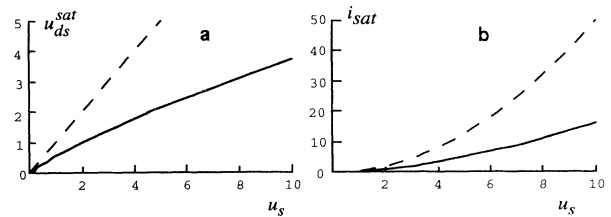


FIG. 4. Saturation voltage (a) and saturation current (b) versus gate voltage swing predicted by the conventional theory (dashed line) and by our theory (solid line). The conventional theory corresponds to the idealized case when the electron saturation velocity  $v_{sat}$  tends to infinity.

We should notice that the steady state in a short-channel FET biased by a dc current source may be unstable with respect to the spontaneous generation of plasma waves (see Ref. 1). However, one can show that the steady state is stable when the FET is biased by a voltage source.

An interesting problem is to establish what should happen at voltages larger than the saturation voltage under the conditions when choking occurs at the drain side of the sample. A similar situation in gas flows involves various complex phenomena (see, for example, Ref. 4) and similar phenomena may be anticipated in the electron fluid in HFET's.

At low voltages,  $eU \ll kT$  (including negative  $U$ ), when the plasma waves become simply sound waves in

the electron fluid with the velocity  $s$  of the order of  $v_{th}$  the relationship  $n_s = CU/e$  is no longer valid, and our theory does not apply. However, the choking phenomenon may still take place so long as  $v_{th}$  and  $v_F$  are less than  $v_{sat}$ . For a short (ballistic) sample ( $L \ll v_{th}\tau$ ), the choking effect will strongly affect the subthreshold  $I$ - $V$  characteristics, reducing the saturation current by a factor  $v_{th}\tau/L$ .

#### ACKNOWLEDGMENTS

This work was partially supported by Advanced Research Project Agency, U.S. Army Research Office, and by U.S. European Army Research Office. We are grateful to M. V. Cheremisin for useful comments.

---

\*Permanent address: A. F. Ioffe, Physico-Technical Institute, St. Petersburg, 194021, Russia.

<sup>1</sup>M. I. Dyakonov and M. S. Shur, *Phys. Rev. Lett.* **71**, 2465 (1993).

<sup>2</sup>R. S. Brodkey, *The Phenomena of Fluid Motion* (Addison-Wesley, Reading, MA, 1967), p. 184.

<sup>3</sup>R. N. Gurzhi, A. I. Kopeliovich, and S. B. Rutkevich, *Adv. Phys.* **36**, 221 (1987); R. N. Gurzhi, A. N. Kalinenko, and A.

I. Kopeliovich, *Phys. Low-Dimensional Struct.* **2**, 75 (1994).

<sup>4</sup>V. L. Streeter and E. B. Wylie, *Fluid Mechanics* (McGraw-Hill, New York, 1985), Chap. 7.

<sup>5</sup>M. S. Shur, *Physics of Semiconductor Devices* (Prentice-Hall, Englewood Cliffs, NJ, 1990).

<sup>6</sup>L. D. Landau and E. M. Lifshitz, *Fluid Mechanics* (Pergamon, New York, 1966).